Current transport and electroluminescence mechanisms in thin SiO$_2$ films containing Si nanocluster-sensitized erbium ions

O. Jambois,[1,a)] Y. Berencen,[1] K. Hijazi,[2] M. Wojdak,[3] A. J. Kenyon,[3] F. Gourbilleau,[2] R. Rizk,[2] and B. Garrido[1]

[1]Dept. Electrònica, MIND-IN2UB, Universitat de Barcelona, Martí i Fanquès 1, 08028 Barcelona, CAT, Spain
[2]CIMAP, UMR CNRS 6252, 6 Boulevard Marchal Juin, 14050 CAEN, France
[3]Department of Electronic and Electrical Engineering, University College London, Torrington Place, London WC1E 7JE, United Kingdom

We have studied the current transport and electroluminescence properties of metal oxide semiconductor (MOS) devices in which the oxide layer, which is codoped with silicon nanoclusters and erbium ions, is made by magnetron sputtering. Electrical measurements have allowed us to identify a Poole–Frenkel conduction mechanism. We observe an important contribution of the Si nanoclusters to the conduction in silicon oxide films, and no evidence of Fowler–Nordheim tunneling. The results suggest that the electroluminescence of the erbium ions in these layers is generated by energy transfer from the Si nanoparticles. Finally, we report an electroluminescence power efficiency above 10^{-3}%. © 2009 American Institute of Physics. [doi:10.1063/1.3213386]

I. INTRODUCTION

There are various methods to obtain electroluminescence (EL) from silicon-based devices, but there is also a need for optimization of devices and better understanding of underlying photogeneration and current transport processes. For the EL signal from silicon-rich silica thin films, the emission is usually attributed to silicon nanocrystals[1,2] or nanoclusters[3,4] (Si-ncls) dispersed in the SiO$_2$ matrix. In order to maximize potential applications, other approaches, including doping stoichiometric silica with rare earth ions, have been studied.[5,6] In most of the cases, the mechanism of conductivity was identified to be Fowler–Nordheim tunneling, and the emission was attributed to impact excitation of the ions by hot electrons. Different strategies are proposed at the device level in order to improve EL efficiency in metal oxide semiconductor (MOS) structure, such as the insertion of a nitride layer to control the energy of injected electrons,[7] or the design of plasmon-enhanced MOS devices.[8]

Because Si-ncls are capable of efficient energy transfer to erbium and other rare earth ions, silicon-rich erbium-doped silica as a material for EL devices became a subject of research.[9–11] However, the role of the Si-ncls in the EL of Er and conduction mechanisms is not clear. It is agreed that the presence of Si-ncls introduces more efficient conduction mechanisms, including variable range hopping,[12] direct tunneling (DT), trap-assisted tunneling, Poole–Frenkel (PF) conduction,[13] or space charged limited current (SCLC).[11] Si nanoparticles favor the injection of charge carriers, improve device lifetime,[14] reduce the population of hot electrons,[15] and consequently reduce impact excitation of Er.[10,16] It has also been argued that other mechanisms of EL can be introduced, including energy transfer from electrically excited Si-

ncls to erbium ions.[13] In general, different processes can be dominant depending on material composition, film thickness, or voltage regimes. An understanding of injection and transport of carriers in erbium-doped silicon-rich silica (SiO$_x$:Er) is a prerequisite to the design of efficient devices.

We have tested a series of MOS structures that enabled us to study the carrier transport and EL from Er^{3+} ions as a function of both silicon and erbium contents. The goal of the present paper is to determine the influence of the Si-ncls on Er EL, on the conductivity of the layers, and on the power efficiency of the device. Finally, our measurements have enabled us to develop a model for the charge transport and EL mechanisms.

II. EXPERIMENTS

The layers were grown on p-type B-doped Si substrates by magnetron cosputtering of three confocal cathodes, SiO$_2$, Er$_2$O$_3$, and Si, under a pure Ar plasma. The rf power applied to each cathode permits the control of the film composition, i.e., the incorporation of Si and Er in the thin layer. More details on the deposition process can be found elsewhere.[17] In total, three different SiO$_x$:Er layers were fabricated, with thicknesses around 30 nm. Thickness was determined by spectroscopic ellipsometry measurements. The layers were annealed at 900 °C for 1 h in nitrogen.

X-ray photoelectron spectroscopy (XPS) spectra were measured with a Perkin-Elmer PHI-5500 instrument using Al $K\alpha$ radiation. XPS depth profiles were obtained by measuring the spectra after sputtering the samples to different thicknesses with an Ar$^+$ ion beam at 4 keV. The time-of-flight secondary ion mass spectrometry (TOF-SIMS) analyses were performed using a TOF-SIMS IV (ION-TOF, Munster, Germany), equipped with a Bi primary ion source, a

TABLE I. Results for Si excess and Er concentration of the four monitor layers.

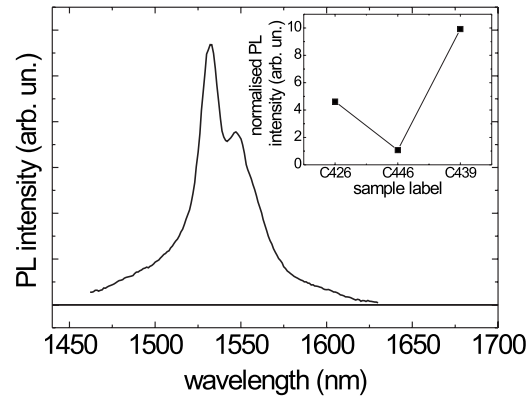| Material	Si excess (%)	Er concentration (at. cm^{-3})	Thickness (nm)
C422	0	1×10^{20}	30
C426	7	4.7×10^{19}	27
C446	18	5.2×10^{20}	35
C439	22	8.4×10^{19}	30

FIG. 1. PL spectrum of sample C446 by indirect pumping of Er. The inset shows the integrated PL intensity normalized to layer thickness and Er concentration for the three Si-rich layers.

Cs/O_2 electron impact dual source column, and a low-energy electron flood gun (for charge compensation of insulating samples).

Photoluminescence (PL) measurements were performed with a DPSS laser emitting at 473 nm, a Bentham M300 single grating monochromator, and a NIR-sensitive Hamamatsu photomultiplier (R5509-72).

The electrical contacts on the back side of the wafers were deposited by successive evaporation of chromium and gold. The top contacts were 60 nm sputtered indium tin oxide (ITO). Different areas from 1.56×10^{-2} to 1 mm^2 were used. To test the transparency of ITO, a series of test samples on glass was prepared, and they showed more than 90% transmission at 1.55 μm. Current-voltage characteristics were performed with an Agilent B1500A semiconductor parameter analyzer. EL measurements were performed with a Hamamatsu G8605 photodiode cooled to -30 °C and a long pass filter with cut-on at 1.4 μm to integrate the light coming from the band at 1.55 μm or an Oriel MS257 monochromator to spectrally resolve the light. The electrical excitation was continuous, not pulsed.

III. RESULTS AND DISCUSSION

A. Structural characterization and PL properties of the layers

XPS measurements were performed to characterize the Si excess. To determine the concentration of Er that is below the resolution of XPS, the sensitive TOF-SIMS technique was used and calibrated with Rutherford backscattering spectroscopy on another SiO_x:Er reference sample. The results for Si excess and Er concentration are given in Table I.

The PL of the four layers was characterized before depositing the electrodes. For each Si-rich layer, a luminescence band at 1.54 μm is observed when pumped at 473 nm, which is clearly attributed to the $^4I_{13/2}$-$^4I_{15/2}$ transition in the internal $4f$ shell of the Er^{3+} ions. A typical PL spectrum can be seen in Fig. 1. As Er is not pumped at a wavelength corresponding to a resonant transition, this suggests that Er ions are indirectly excited by the Si-ncls thanks to energy transfer, as proposed in literature.[18,19] In the inset of Fig. 1, the PL intensity of the three Si-rich samples has been normalized to the layer thickness and the Er concentration. Different intensities are found, but no clear dependence on Si excess or Er concentration can be inferred. These differences in PL intensities are attributed either to different fractions of optically active Er in the layers, or a different fraction of Er ions coupled to Si-ncls. The fact that the layer with the higher Er content has the lower PL intensity suggests also that for this layer there is some Er agglomeration.

B. Conduction and EL properties

In Fig. 2, we present a typical *J-V* characteristic obtained for one device in both polarities. By convention, positive voltage to the *p*-type substrate corresponds to forward polarization. It can be seen that the current increases by several orders of magnitude over the range of voltages used here, which is typical of strong insulators. At lower voltages, the *J-V* curves are symmetric for both polarities, which suggests that the current is limited by the bulk of the active layer, and not by the electrode.[20] However, note that this is not true at higher voltages, as a saturation of the current can be observed in reverse polarization. This can be attributed to the lower density of electrons in the *p*-type substrate in inversion that can be injected in the dielectric so the injection becomes interface limited.

In the inset of Fig. 3, we present an EL spectrum showing an EL band at 1.55 μm, which is clearly attributable to the Er ions in the active layer. Note that the EL spectrum appears broader than the PL spectrum as for EL the slits of the monochromator were opened to the maximum to detect as much light as possible. This leads to a higher signal but lower resolution and a broadening of the spectrum. This kind of spectrum was obtained for samples that contain excess Si (C426, C446, and C439) when in forward bias. As can be
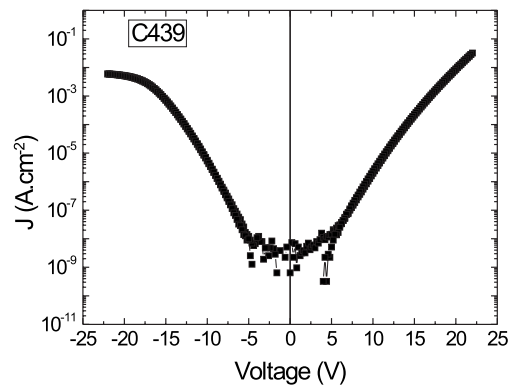

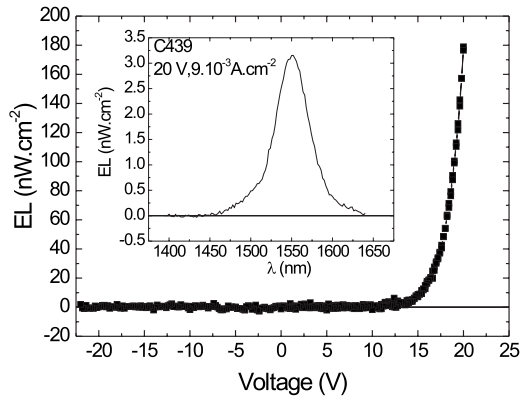FIG. 2. *J-V* characteristic of sample C439.

FIG. 3. EL power vs voltage of sample C439. The inset shows an EL spectrum

seen in Fig. 3, the EL intensity increases with the applied voltage. Under negative voltage, no EL was observed. It is also worth mentioning that sample C422, which has no Si excess, does not show any EL at 1.55 μm for any polarization.

In order to understand the conduction mechanisms, we present in Fig. 4(a) the current density–electric field (*J-E*) characteristics of the four samples. The electric field, given by the voltage divided by the active layer thickness, has been increased as much as possible before seeing breakdown of the device. In Fig. 4(a), we can see a strong variation of the current with applied field, in particular for the Si-rich samples (C426, C439, and C446). Moreover, the current is
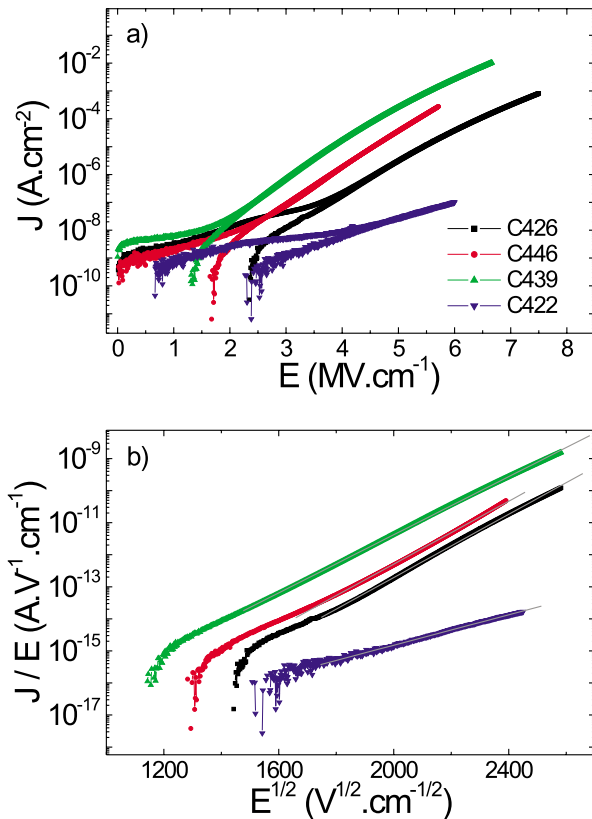

FIG. 4. (Color online) *J-E* characteristics of the layers (a) in log scale and (b) in PF representation. The legend that appears in (a) applies for both pictures.

strongly enhanced when a Si excess is introduced in the silicon oxide, as the current is increased by four or five orders of magnitude. This shows that the transport of charges occurs through the Si nanoparticles. This is also supported by the increase in conductivity with Si excess. If we compare the current densities to the ones given by other groups on similar materials made by sputtering,[11] the values found in the present study are much lower. This could suggest that the layer we have fabricated contains fewer matrix defects, leading to a lower conductivity.

Different models are known to describe current transport in silicon oxides through defects—for example, phonon-assisted tunneling, DT, field assisted thermal ionization, or SCLC.[20,21] The first two correspond to tunnel escape of charges from trap to trap. At higher electric fields, transport is generally well described by the Fowler–Nordheim mechanism, which corresponds to injection of charges from the electrode into the conduction band of the dielectric by tunneling through a triangular potential barrier. In our case, the data for the Si-rich samples are best described by the PF model, that is to say, the field-enhanced thermal emission of carriers from trapping sites in the insulator. This law is generally described by the following equation:

$$J \propto E \times \exp\left(\frac{1}{kT} \sqrt{\frac{e^3 E}{\pi \varepsilon_0 \varepsilon_r}} \right),$$

where kT is the thermal energy, e is the electron charge, ε_0 is the vacuum permittivity, and ε_r is the relative permittivity of the film.[20] From the fit, the value of ε_r can be deduced. From the effective medium theory, the value of ε_r can vary between 4 and 12, corresponding to the permittivities of SiO_2 and of pure Si, respectively. Figure 4(b) shows the *J-E* curve in the PF representation, i.e., the logarithm of the ratio J/E versus the square root of E. A straight line in a large range of J/E can be found for the Si-rich samples, giving values of permittivity consistent with the effective medium theory. For samples C426, C446, and C439, values of permittivity of 6.6, 6.9, and 7.9 were found. The increasing value of the permittivity with the Si excess is further evidence of the role of the Si-ncls in charge transport. The dominance of this mechanism in these kinds of layers is in agreement with what has previously been reported,[13,14,21] but contradicts other results,[11] in which a SCLC-type mechanism and much higher current density current even at low electric field were reported. We attribute this difference to the lower matrix defect density in the samples presented here than in Ref. 11, consistent with the lower currents we measure. It was also intended to fit the *I-V* characteristics with the Fowler–Nordheim law discussed above. In principle this kind of mechanism can lead to the injection of hot electrons in the active layer. This process is well known to be dominant for silicon oxides or silicon oxides with Si-ncls at high electric fields, when the films contain a much lower content of matrix defects. For example, we reported that layers of thermal SiO_2 implanted with Si and annealed at high temperature show good agreement with Fowler–Nordheim injection, and the EL mechanism of excitation of the Si-ncls was attributed to impact ionization.[22] This is also the case reported by Nazarov *et al.*,[10] who observed a Fowler–Nordheim-type injec-

tion in SiO_x:Er layers that have been fabricated by sequential implantation of Si and Er in a SiO_2 layer made by thermal oxidation of a Si substrate. In this study, the higher density of defects due to the preparation method seems to favor the injection of charges inside the dielectric, preventing hot electron injection, when the electric field is not too high. In the case of sample C422 (no silicon excess), different behavior is observed. Although the fit with the PF model seems reasonable, a permittivity of about 20 is found. This suggests that a mechanism of thermal ionization assisted by electric field could occur, but with some differences. In fact, a better fit with the SCLC mechanism could be found. This law is generally well fitted by a power dependence of I with V. In the ideal case, the exponent is equal to 2, as can be analytically found if we consider a dielectric free of traps or with shallow traps situated at a constant energy below the conduction band. In the case of a distribution of deeper states, higher values of exponent can be found.[23] In our case, an exponent of 7 has been found, which suggests that the defects present in the layers that assist conduction show a large energy distribution; this is understandable as the medium is essentially amorphous.

The power efficiency of EL is defined as the ratio between the power of the emitted light and the input electrical power. This value has been estimated for the three Si-rich layers by carefully calibrating the EL setup. We obtained power efficiencies of $2.3 \times 10^{-4}\%$, $1.2 \times 10^{-3}\%$, and $1.1 \times 10^{-4}\%$, for samples C426, C446, and C439, respectively. There is no clear tendency that appears with Si excess or Er concentration. This is because the system is governed by several parameters, including the Si-ncl density and the fraction of coupled Er. In fact, the EL results are contrary to the PL results of Fig. 1; i.e., the sample with the highest PL intensity has the lowest EL power efficiency. Actually, PL and EL do not necessarily coincide as, on one hand, for optical pumping the luminescent centers have to be well isolated to ensure the best confinement, whereas for electrical pumping the luminescent centers have to be close to one another to allow charge transport.[11,24] Moreover, even if the layers can be optimized by PL in terms of Er coupled to Si-ncls, we have to deal with different paths for the flow of charges, which can be matrix defects, Si-ncls not coupled to Er ions, or Si-ncls that are coupled to the Er ions. Among these three, only the last one allows excitation of Er, and the samples have to be prepared in order to favor this mechanism. The low matrix defect density has allowed us to obtain a power efficiency of $1.2 \times 10^{-3}\%$ for the best result, corresponding to an external quantum efficiency of 0.03%. In general, authors only report external quantum efficiency, which is the upper limit for power efficiency,[25] but power efficiency values are the one required for application purposes. To our knowledge, the value of power efficiency we report is the highest reported in Si-ncl sensitized Er ion systems. One expects a significant increase in this number for optimized material that is currently the object of intense effort.

C. Excitation mechanisms

Having clearly demonstrated the role of Si-ncls in the enhancement of the conductivity of the stoichiometric layer,
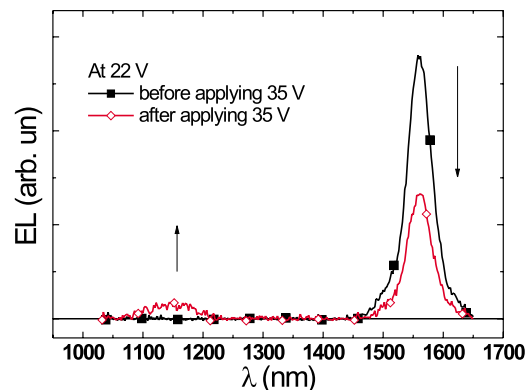

FIG. 5. (Color online) EL spectrum from 1000 to 1700 nm at 22 V before applying 35 V (full squares) and after applying 35 V (empty diamonds).

we have studied the mechanism of Er excitation. We can imagine three scenarios that may occur in those layers leading to excitation of the Er ions: (i) impact ionization of Er directly, so the Si-ncls act only as paths for conduction; (ii) impact ionization of the Si-ncls and transfer of the excitonic energy to the nearest Er; or (iii) injection of electron and hole in the same Si-ncls, formation of an exciton, and transfer to the closest Er. In the case of impact ionization, the electron needs to reach a high kinetic energy. When it is high enough, the collision of this electron with a Si-ncl allows the creation of an exciton confined inside the Si-ncls, which can transfer its energy to the Er ions. Also, the hot electron can excite Er directly by collision. If the electron does not collide with the scattering centers (Si-ncls, Er, and matrix defects), it will impact the Si substrate. Thus, if hot electrons can be created by field ionization, radiative emission of the Si substrate due to impact ionization should be observable. In Fig. 5, an EL spectrum has been measured from 1 to 1.7 μm, to observe luminescence of Er at 1.55 μm, and that from the Si substrate at around 1.15 μm. The spectrum is measured at a bias of 22 V, and the device has never previously been subjected to voltages larger than 22 V. By increasing the electric field the EL intensity at 1.55 μm increases, as has already been seen in Fig. 3. However, when the applied voltage becomes higher than 35 V, the EL at 1.55 μm drops suddenly, and a new band appears at 1.15 μm. At the same time, the current shows also a noticeable increase (not shown). When reducing the bias to 22 V, the spectrum remains changed across the whole measured range, as can be seen in Fig. 5; the new band at 1.15 μm remains, and the EL of Er is lower.

In Fig. 5, before applying voltages higher than 35 V, no luminescence from the Si substrate is observed, suggesting that hot electrons are not injected in the active layer. This is supported by the fact that no Fowler–Nordheim injection was observed. Instead, the charges are trapped by the matrix traps (Si-ncls or matrix defects) with a high probability because of their high density. If the electrons increase their kinetic energy (become hot) due to the electric field, they would thermalize very quickly. This suggests that the light emitted from Er does not come from impact ionization either of Er or of the Si-ncls. It appears more likely that in these layers we see bipolar injection of electrons from the ITO electrode and of holes from the accumulation region in the Si
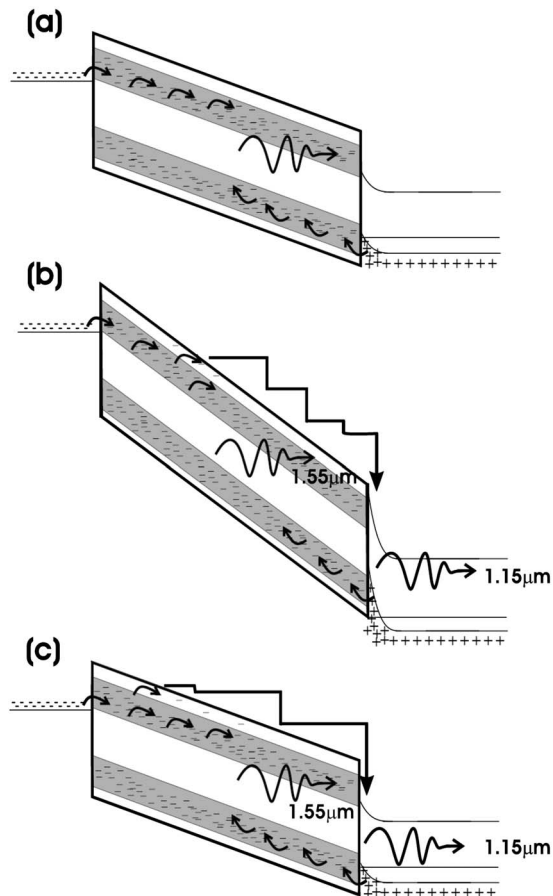
(a)

(b)

1.55 μm

1.15μm

(c)

1.55μm

1.15μm

FIG. 6. Energy diagrams of the ITO/SiO_x:Er/p-Si structure. (a) At low voltage before applying 34 V, (b) at higher voltage, and (c) back to low voltage.

substrate into the Si-ncls, and that a transfer of the excitonic energy to the Er ions occurs. The fact that no EL is observed in reverse polarization suggests that holes are necessary to obtain Er EL. Moreover, another indication of the indirect excitation of Er is the fact that the SiO_2:Er layer does not show any EL. If we now consider the regime where very high electric fields are applied to the device—close to the layer breakdown—additional traps can be generated by the applied field. These new traps constitute a new channel for the conduction of charges, leading to a higher current, and some of the charges can reach the conduction band of the matrix. As the mobility is much higher there, electrons can remain hot and reach the Si substrate. This explains the appearance of a luminescence band at 1.15 μm. Finally, when coming back to 22 V, the defects generated by the high electric field are still there; hence it is still possible to generate hot electrons and the EL band due to the Si substrate remains. The decrease in the intensity of the EL band could be due either to a lower fraction of charges that flow through the traps inside the gap, or to a nonradiative interaction between excitons and hot electrons (Auger).

From all the above results, we propose a model describing the conduction of charges in our sample for different regimes of electric field, and explaining the different EL bands emitted from the device. We schematize in Fig. 6(a) the mechanism in an energy-space diagram at low voltage.

The active layer in the center is sandwiched between the ITO semimetallic electrode and the p-type Si substrate. The high density of traps characterizing the films (Si-ncls or matrix defects) allows conduction of charges with a reduced mobility compared to an electron in the conduction band, and hence a PF mechanism occurs. At low voltages in forward bias, electrons are injected from the ITO electrode, and holes from the Si substrate. EL from Er can be observed: we symbolize it by the twisted arrow in the center of the active layer. When a higher voltage is applied, the electric field is close to breakdown [see Fig. 6(b)], and it is likely that defects are created inside the layer. The charges follow these new channels, and are injected into the conduction band of the silicon oxide matrix. There the electrons can become hot, as they suffer less scattering than in the pseudoconduction band created in the gap of the oxide. They are thus able to impact with the substrate, and this explains the luminescence of the substrate that appears at high fields, as observed in Fig. 5, as well as the observed increase in the current intensity. Finally, when coming back to lower field [see Fig. 6(c)], the defects created by the high electric field are still there, and charges can still be injected into the conduction band of the matrix. This leads to a new situation in which a new luminescence band appears at 1.15 μm. As a fraction of electrons are deviated from their original trajectory, less EL at 1.55 μm is obtained.

IV. CONCLUSIONS

In summary, we have studied the conduction and EL mechanisms in SiO_x:Er layers of different compositions, as well as their power efficiency. The presence of Si-ncls leads to an increase in the current of four to five orders of magnitude. The conduction mechanism is found to be dominated by field assisted thermal ionization (PF) from Si-ncls to Si-ncls. At lower voltages, no evidence of hot electron injection has been seen. The experiments allow us to attribute the erbium EL to a transfer of the excitonic energy of the Si-ncls to Er ions, and to discount impact ionization of either the Si-ncls or Er ions. A power efficiency above 10^{-3}% has been found for the best device. A model is proposed to explain the different regimes of luminescence with the applied voltage that occurs in these devices.

[1]G. Franzò, A. Irrera, E. C. Moreira, M. Miritello, F. Iacona, D. Sanfilippo, G. Di Stefano, P. G. Fallica, and F. Priolo, Appl. Phys. A: Mater. Sci. Process. **74**, 1 (2002).
[2]R. J. Walters, G. I. Bourianoff, and H. A. Atwater, Nature Mater. **4**, 143 (2005).
[3]A. Irrera, F. Iacona, I. Crupi, C. D. Presti, G. Franzò, C. Bongiorno, D. Sanfilippo, G. Di Stefano, A. Piana, P. G. Fallica, A. Canino, and F. Priolo, Nanotechnology **17**, 1428 (2006).
[4]V. Filip, H. Wong, C. K. Wong, and D. Nicolaescu, J. Vac. Sci. Technol. B **26**, 813 (2008).
[5]S. Prucnal, J. M. Sun, W. Skorupa, and M. Helm, Appl. Phys. Lett. **90**,

181121 (2007).

[6]H. Jeong, S.-Y. Seo, and J. H. Shin, Appl. Phys. Lett. **88**, 161910 (2006).

[7]M. Perálvarez, J. Carreras, J. Barreto, A. Morales, C. Domínguez, and B. Garrido, Appl. Phys. Lett. **92**, 241104 (2008).

[8]A. Hryciw, Y. C. Jun, and M. L. Brongersma, Opt. Express **17**, 185 (2009).

[9]F. Iacona, D. Pacifici, A. Irrera, M. Miritello, G. Franzò, F. Priolo, D. Sanfilippo, G. Di Stefano, and P. G. Fallica, Appl. Phys. Lett. **81**, 3242 (2002).

[10]A. Nazarov, J. M. Sun, W. Skorupa, R. A. Yankov, I. N. Osiyuk, I. P. Tjagulskii, V. S. Lysenko, and T. Gebel, Appl. Phys. Lett. **86**, 151914 (2005).

[11]K. Sun, W. J. Xu, B. Zhang, L. P. You, G. Z. Ran, and G. G. Qin, Nanotechnology **19**, 105708 (2008).

[12]M. Fujii, Y. Inoue, S. Hayashi, and K. Yamamoto, Appl. Phys. Lett. **68**, 3749 (1996).

[13]F. Priolo, C. D. Presti, G. Franzò, A. Irrera, I. Crupi, F. Iacona, G. Di Stefano, A. Piana, D. Sanfilippo, and P. G. Fallica, Phys. Rev. B **73**, 113302 (2006).

[14]S. Prezioso, A. Anopchenko, Z. Gaburo, L. Pavesi, G. Pucker, L. Vanzetti, and P. Bellutti, J. Appl. Phys. **104**, 063103 (2008).

[15]D. J. DiMaria, T. N. Theis, J. R. Kirtley, F. L. Pesavento, D. W. Dong, and S. D. Brorson, J. Appl. Phys. **57**, 1214 (1985).

[16]M. E. Castagna, S. Coffa, M. Monaco, L. Caristia, A. Messina, R. Mangano, and C. Bongiorno, Physica E (Amsterdam) **16**, 547 (2003).

[17]K. Hijazi, L. Khomenkova, J. Cardin, F. Gourbilleau, and R. Rizk, Physica E (Amsterdam) **41**, 1067 (2009).

[18]A. J. Kenyon, P. F. Trwoga, M. Federighi, and C. W. Pitt, J. Phys.: Condens. Matter **6**, L319 (1994).

[19]M. Fujii, M. Yoshida, Y. Kanzawa, S. Hayashi, and K. Yamamoto, Appl. Phys. Lett. **71**, 1198 (1997).

[20]S. M. Sze, *Physics of Semiconductor Devices*, 2nd ed. (Wiley, New York, 1981).

[21]J. G. Simmons, Phys. Rev. **155**, 657 (1967).

[22]O. Jambois, A. Vilà, P. Pellegrino, J. Carreras, A. Pérez-Rodríguez, B. Garrido, C. Bonafos, and G. BenAssayag, J. Lumin. **121**, 356 (2006).

[23]R. M. Hill, Thin Solid Films **1**, 39 (1967).

[24]P. M. Fauchet, Mater. Today **8**, 26 (2005).

[25]B. Gelloz and N. Koshida, J. Appl. Phys. **88**, 4319 (2000).